Photochemical Aging of Secondary Organic Aerosols Generated from the Photooxidation of Polycyclic Aromatic Hydrocarbons in the Gas-Phase

ARTICLE *in* ENVIRONMENTAL SCIENCE & TECHNOLOGY · APRIL 2015

Impact Factor: 5.33 · DOI: 10.1021/acs.est.5b00442 · Source: PubMed

5 AUTHORS, INCLUDING:

Ellis Shipley Robinson

University of Colorado Boulder

8 PUBLICATIONS **89** CITATIONS

SEE PROFILE

Neil M Donahue

Carnegie Mellon University

271 PUBLICATIONS **10,599** CITATIONS

SEE PROFILE

Environmental Science & Technology

Article

pubs.acs.org/est

Photochemical Aging of Secondary Organic Aerosols Generated from the Photooxidation of Polycyclic Aromatic Hydrocarbons in the Gas-Phase

Matthieu Riva,[†,‡,∥] Ellis S. Robinson,[§] Emilie Perraudin,[†,‡] Neil M. Donahue,*[,§] and Eric Villenave*[,†,‡]

[†]University of Bordeaux, EPOC, UMR 5805, F-33405 Talence cedex, France

[‡]CNRS, EPOC, UMR 5805, F-33405 Talence cedex, France

[§]Center for Atmospheric Particles Studies, Carnegie Mellon University, Pittsburgh, Pennsylvania 15213, United States

Supporting Information

ABSTRACT: Aging processes of secondary organic aerosol (SOA) may be a source of oxygenated organic aerosols; however, the chemical processes involved remain unclear. In this study, we investigate photochemical aging of SOA produced by the gas-phase oxidation of naphthalene by hydroxyl radicals and acenaphthylene by ozone. We monitored the SOA composition using a high-resolution time-of-flight aerosol mass spectrometer. We initiated SOA aging with UV photolysis alone and with OH radicals in the presence or absence of light and at different NO_x levels. For naphthalene, the organic composition of the particulate phase seems to be dominated by highly oxidized compounds such as carboxylic acids, and aging data may be consistent with diffusion limitations. For acenaphthylene, the fate of oxidized products and the moderately oxidized aerosol seem to indicate that functionalization reactions might be the main aging process were initiated by the cumulative effect of light and OH radicals.

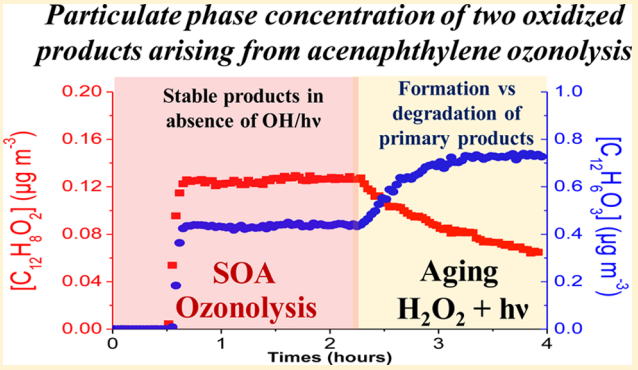

INTRODUCTION

Atmospheric fine particulate matter (PM) plays a key role in air quality and climate change and is associated with damaging effects on human health.[1,2] Organics are a major fraction of PM, comprising up to 90% of the fine PM mass.[3] Even in urban areas, organic aerosol is dominated by secondary organic aerosol (SOA).[2] SOA mainly results from the formation of low vapor-pressure products, arising from the oxidation of volatile organic compounds (VOCs).[2] Numerous recent field measurements have measured large concentrations of oxygenated organic aerosols (OOA).[4] Although OOA is generally equated with SOA, two challenges confound this association: many models underpredict observed OOA concentrations, and both SOA formation experiments and models fail to predict the degree of oxidation in ambient OOA observations. Some form of oxidative aging chemistry is thought to be responsible for these differences.[5−7] To elucidate the chemical processes involved in SOA aging, numerous studies have been recently reported.[8−12]

Different chemical processes could be involved in aging reactions. Heterogeneous oxidation in the presence of hydroxyl radicals (OH) or ozone (O_3) is one possibility. Photolysis or multiphase reactions should also influence the bulk composition of organic aerosol. Functionalization, fragmentation, and accretion pathways have been previously identified in the particulate phase.[3,13] However, branching among the different pathways may be quite variable depending on ambient or experimental conditions.[14] Aging will certainly alter the chemical composition of aerosol particles, and this in turn may well influence physicochemical properties such as volatility, hygroscopicity, viscosity, and optical properties.[15,16] Understanding SOA aging at a molecular level is necessary for improved knowledge of the impact of OOA and of the chemical processes involved in their formation, and for this to be implemented in chemistry transport models. Indeed, SOA chemistry in most chemical models is based on parametrizations from smog-chamber data, where experiments are performed for only few hours and often consider only one oxidant (excluding potential cocktail effects); this induces a gap between atmospheric reality and experiments.

Aging processes including multiple oxidation steps and multiple oxidants are still rarely implemented in atmospheric models. Recently, some studies have demonstrated the importance of different processes on the SOA composition and mass such as photolysis of particle matter or OH radical

Received: April 14, 2014
Revised: April 7, 2015
Accepted: April 9, 2015
Published: April 9, 2015

DOI: 10.1021/acs.est.5b00442
Environ. Sci. Technol. 2015, 49, 5407−5416

oxidations of organic vapors.[9,10] Moreover, current models still often predict less SOA than typically observed during field measurements.[2,14] A large part of this underestimation is due to the lack of consideration of some SOA precursors, including intermediate volatility organic compounds (IVOC), such as alkanes or polycyclic aromatic hydrocarbons (PAHs).[17] Substantial effort in the research community is focused on identifying this missing or misrepresented source of SOA.

Polycyclic aromatic hydrocarbons (PAHs) are one of the major classes of anthropogenic emissions and are potentially carcinogenic and mutagenic.[18−20] Some recent studies have reported the SOA mass yields from oxidation of PAHs by different atmospheric oxidants.[21−26] In parallel, studies focusing on the aging of monoaromatic-derived aerosols found large concentrations of carboxylic acids or hydroxycarbonyl compounds present in the particulate phase.[12,27] Although these aging studies demonstrated an increase of the O/C ratio, the aged SOA was still less oxidized than ambient OOA.

This work presents the first study specifically focusing on the aging of SOA generated from gaseous PAH oxidation. Our objective is to investigate different chemical processes influencing the evolution of the particulate phase during the formation and aging of SOA arising from the oxidation of naphthalene and acenaphthylene via photolysis and OH radical reactions. Naphthalene has some of the highest emissions among gaseous PAHs found in the atmosphere and has been used as a model for anthropogenic precursors in smog-chamber experiments.[27,28] The SOA mass yields reported in the literature demonstrated the potential contribution of PAHs to the SOA budget, especially in urban areas.[21,26,29] Acenaphthylene is also emitted in the gas phase and, due to its structure (it contains a C═C double bond), it presents a specific reactivity with several atmospheric oxidants.[19] Indeed, its reaction kinetics with ozone or nitrate radicals is very fast.[25,26,30] SOA yields, chemical composition in both gaseous and particulate phases have recently been described in studies on the photooxidation of naphthalene (involving OH) and the ozonolysis of acenaphthylene.[21−26,30]

EXPERIMENTAL SECTION

General Conditions of Experiments in Smog Chamber and Analytical Setup. Experiments were performed in the environmental smog chambers of Center for Atmospheric Particles Studies (CAPS) at Carnegie Mellon University. The experimental setup and analysis techniques used in this work were described in detail previously[31] and is defined in the Supporting Information (SI). Briefly, experiments were carried out at (295 ± 1) K under dry conditions (RH was below 10%) in 10 m^3 and 12 m^3 Teflon chambers surrounded by UV lamps. The lights in the CMU chamber have a distinct peak at 350 nm. SOA formation was carried out in the presence of ammonium sulfate seed particles and 2 ppm ozone, with tetramethylethylene (TME) added to produce OH radicals for naphthalene oxidation.[32] Naphthalene (Sigma-Aldrich, 99%) or acenaphthylene (Sigma-Aldrich, 99%) was introduced into the chamber by passing dry purified air over a heated Pyrex glass bulb containing a known amount of solid compound. Typical initial PAH concentrations were 50 and 40 ppb for naphthalene and acenaphthylene, respectively. Aging was carried out with UV illumination alone or by adding various OH precursors, including TME, HOOH, and HONO. Experimental conditions are summarized and described in SI Table S1.

We used a Scanning Mobility Particle Size Spectrometer (SMPS, TSI 3936) to measure particle number distributions and a high-resolution time-of-flight aerosol mass spectrometer (HR-AMS, Aerodyne) to characterize the particle phase composition and its evolution.[33] The HR-AMS uses 70 eV electron-impact ionization following 600 °C thermal vaporization for accurate measurement of bulk OA composition with high time resolution, but for most species the resulting fragmentation and complex organic aerosol composition obscures measurement of individual species. However, aromatics and especially PAHs are resistant to fragmentation and show strong signals at the parent m/z.[34] It is thus possible to associate high m/z signals in the AMS with specific molecular structures and not just molecular fragments, though whether these structures exist in the particles as monomers or components of higher molecular weight species (oligomers) is not certain. Consequently, we shall discuss high time resolution measurements of many important specific particulate-phase products attributed to high m/z signals.

SOA Formation. In the case of naphthalene, SOA formation was initiated by its reaction with hydroxyl radicals. In order to first isolate the influence of UV light on SOA formation, OH radicals were formed from the ozonolysis of tetramethylethylene (TME, Matheson) in darkness and subsequently under UV illumination. As shown in many studies, TME ozonolysis is a convenient dark OH radical source for aging experiments,[10,32] and the added (∼350 nm) UV in this case should not have a first-order effect of OH generation. After naphthalene injection, ozone was introduced in large excess (2 ppm) in the chamber by flowing O_2 from an oxygen tank through an ozone generator. The reactivity of naphthalene with ozone is too slow (2×10^{-19} cm^3 $molecule^{-1}$ s^{-1}) to cause observable reaction between these two species in our system,[35] and indeed we observed none. A continuous flow of TME (1×10^9 molecules cm^{-3} s^{-1}) was then introduced to the chamber. Lambe et al.[32] have previously calibrated OH production from TME ozonolysis. Under the conditions we employed, the concentration of OH radicals was expected to be $4-8 \times 10^6$ molecules cm^{-3} as previously measured by Lambe et al.[32]

Immediately after TME injection, naphthalene oxidation commenced, and we observed SOA formation. Particle growth was monitored using an SMPS in addition to the HR-AMS. Volume and number concentrations were measured for aerosols over the (mobility) diameter range 15−700 nm. Complete depletion of naphthalene took around 2 h, based on stabilization of the particle volume modal diameter. The naphthalene lifetime for a conservatively estimated OH radical concentration of 6×10^6 molecules cm^{-3} was 2 h based on a rate coefficient for the reaction of naphthalene with OH of 2.3×10^{-11} cm^3 $molecule^{-1}$ s^{-1}.[36] Thus, the naphthalene should be consumed after 2 h. At this point, OH radical formation was stopped by switching off the TME injection, and the system was held in the dark for 2 h.

Acenaphthylene is highly reactive with ozone.[25,30] Thus, SOA formation was directly initiated by acenaphthylene ozonolysis without injection of TME. Two ppm of ozone was used to facilitate subsequent aging experiments. The lifetime of acenaphthylene was 50 s for these conditions, based on a reaction rate constant with ozone of 4.0×10^{-16} cm^3 $molecule^{-1}$ s^{-1}.[30] Although acenaphthylene ozonolysis was fast compared to typical atmospheric conditions, it was necessary to use high concentration of O_3 in order to keep

DOI: 10.1021/acs.est.5b00442
Environ. Sci. Technol. 2015, 49, 5407−5416

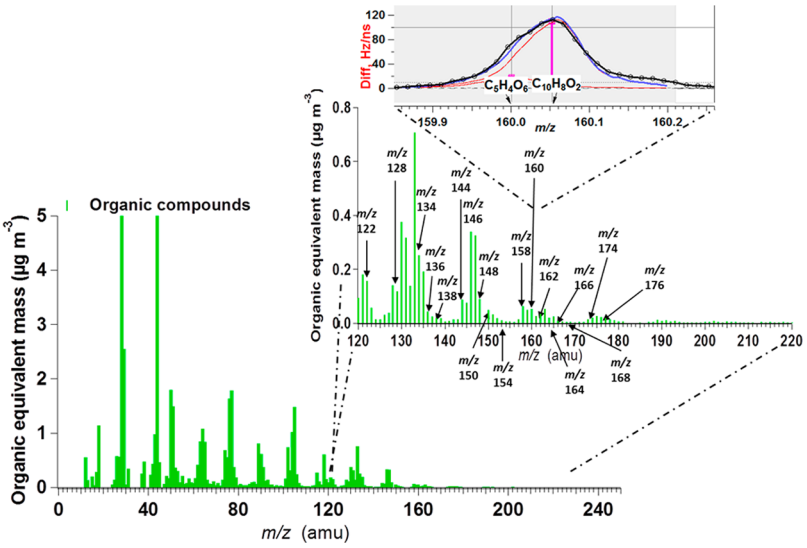

Figure 1. Mass spectra obtained during naphthalene oxidation and corresponding mass fragments of identified products. An example of HR-AMS fit for fragment m/z 160 is proposed and demonstrates a very good agreement between signal at the mass 160 and proposed structure of formylcinnamaldehyde (other fit for different fragments are presented in the SI).

the steady-state TME levels low during aging and thus prevent TME itself from consuming most of the OH.[32] No significant OH radical formation arising from acenaphthylene ozonolysis have been demonstrated in previous studies.[25,30] Thus, additional oxidation process is assumed negligible during SOA formation from acenaphthylene ozonolysis.

Aging Experimental Protocol. We conducted a series of experiments to investigate aging driven by UV light and oxidants (summarized in SI Table S1). Although the SOA formation processes for naphthalene and acenaphthylene differed as described above, the conditions for aging experiments were similar. To investigate the impact of various OH radical concentrations in different conditions, we used nitrous acid (HONO), hydrogen peroxide (H_2O_2), and TME + ozone as OH sources:

We used HONO UV photolysis to generate OH radicals and nitrous oxide (NO), creating high-NO_x conditions and high OH concentrations. The OH radical concentration during the first hour of HONO photolysis was $1-2 \times 10^7$ molecules cm^{-3}. After depletion of a large proportion of the HONO in roughly 1 h, the OH concentration relaxed to around 10^6 molecules cm^{-3}. We used H_2O_2 UV photolysis to investigate the impact of OH radicals and hydroperoxyl radical (HO_2) in the absence of NO_x. The OH concentration was stable near 10^6 molecules cm^{-3}. In the case of HONO and H_2O_2, two sets of calibration were performed using a GC-FID to monitor the depletion of 2-butanol and quantify the OH radical production from the HONO and H_2O_2 photolysis. TME ozonolysis was used to separate the impact of OH radicals from that of light during SOA aging. OH radical concentrations were in this case $4-8 \times 10^6$ molecules cm^{-3}. This source was employed in the dark and also in under UV illumination to explore the effect of photolysis on SOA aging. Finally, we performed aging experiments using UV light alone to investigate the impacts of photolysis on SOA composition.

RESULTS AND DISCUSSION

SOA Formation. First we shall discuss product formation during the first portion of paired experiments, before SOA aging. Various products were identified in the particle phase using HR-AMS during acenaphthylene ozonolysis and the OH-initiated oxidation of naphthalene. Indeed, as presented in Figure 1 and in SI Figures S1 to S3 oxidized products arising from PAH oxidation can be observed using HR-AMS. We verified that the proposed chemical structures (SI Tables S1 and S2) were consistent with the identified fragments using high-resolution mass spectral analysis (SI Figures S2 and S3), that were processed using the toolkits Squirrel, version 1.52, and Pika, version 1.11 (http://cires.colorado.edu/jimenezgroup/wiki/index.php/ToF-AMS_Analysis_Software). Most of these compounds have already been identified in previous studies using different online and offline techniques, and chemical mechanisms have also been proposed.[22−26,30] For SOA derived from both acenaphthylene and naphthalene SOA, we observed a significant signal at an m/z value corresponding to the parent ion of each SOA precursor, although partitioning considerations suggest that the activity of each PAH in the SOA should be very small. It is thus not known whether the molecules observed in the AMS data correspond directly to monomers in the SOA or potentially to fragments of higher molecular weight association products, but as we shall show interpretation of these signals in terms of monomer products makes mechanistic sense.

Most of the identified products arising from naphthalene oxidation are ring-opening products and are highly oxidized compounds like acidic compounds, as already demonstrated by previous study.[22−24] They account for a large fraction of the characterized particle phase. As presented in SI Figure S4, no difference between identified naphthalene particulate products has been observed for experiments performed in the presence of light or in darkness. Therefore, photolysis seems to have a negligible impact on products adsorbed at the surface of SOA.

In the case of acenaphthylene ozonolysis, we compare the first 2 h of experiments Exp#A3 and Exp#A5 in Figure 2. In each case, SOA was formed very quickly (consistent with the extremely short acenaphthylene lifetime), and there was no significant difference in the total mass concentration of SOA in the dark or in the presence of UV light. However, the concentrations of the different identified products depended on the oxidation conditions during SOA formation (i.e., the

DOI: 10.1021/acs.est.5b00442
Environ. Sci. Technol. 2015, 49, 5407−5416

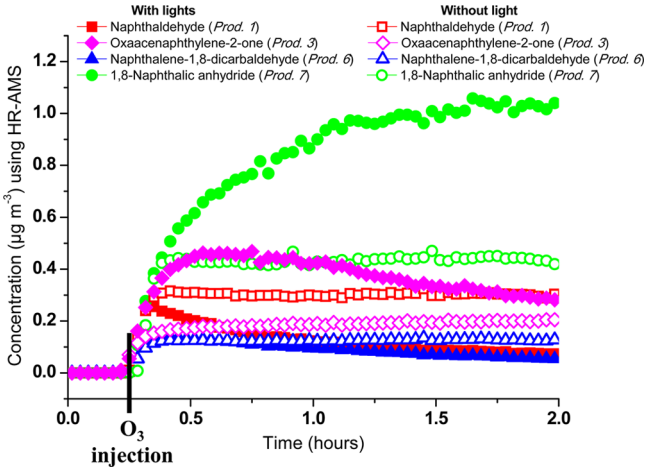

Figure 2. Particulate phase profiles of acenaphthylene ozonolysis products formed in darkness (Exp#A3, open markers) and in the presence of UV light (Exp#A5, filled markers).

absence or presence of UV light). Before SOA generation, no organic compound was identified in the particulate phase, indicating that no condensation of acenaphthylene occurred on seed particles, consistent with expectations. For dark ozonolysis, the identified compounds (SI Table S2) generally showed quite constant signal levels after the rapid SOA formation. Most, such as those shown with open symbols in Figure 2 (**Products 1**, **3**, **6**, 7), showed no change at all. However, the SOA composition after dark ozonolysis was largely consistent with minimal chemical evolution following the initial SOA formation.

Ozonolysis in the presence of UV light led to much different behavior, in spite of the nearly identical total SOA mass concentration. Some species were gradually depleted over the 2-h incubation period while others gradually increased, as shown in Figure 2 (filled symbols) Naphthaldehyde (**Product 1**) and oxaacenaphthylene-2-one (**Product 3**) were depleted, whereas, 1,8-naphthalic anhydride (**Product 7**) was continuously formed during SOA formation. In other cases, species such as **Products 1** and **3** showed signs of competition between generation by the photooxidation of primary products (e.g., naphthalene-1,8-dicarbaldehyde)[26] and subsequent depletion. Such observations have already been reported in a recent study by our group,[25,26] allowing us to tentatively propose a chemical mechanism describing the complex reaction system. We shall discuss these data in the "aging" section below.

Aging of SOA Arising from Naphthalene Oxidation. One technique to characterize the evolution of bulk OA properties during aging is the "triangle plot" introduced by Ng et al.[4] Fragments m/z 43 and m/z 44 are the dominant ions in oxidized organic aerosol (OOA) spectra and represent different functional groups. The organic mass fraction f_{44} (defined as the organic particle signal at m/z 44 normalized to the total organic particle mass) is dominated by CO_2^+ moiety. Previous studies have demonstrated that CO_2^+ from AMS spectra is related to decarboxylation of organic acidic groups.[4] The organic mass fraction f_{43} (defined as the organic particle signal at m/z 43 normalized to the total organic particle mass) is dominated in the case of naphthalene by the $C_2H_3O^+$ fragment and indicative of nonacid oxygenated functional groups such as aldehydes, ketones or alcohols.[12,27,37]

In Figure 3 we show a triangle plot for different naphthalene aging experiments along with the triangular region typical of ambient samples in the inset. All of the data lie outside and to the left of the ambient range (with lower f_{43}) but also show monatomic increases in f_{44} during aging. It is not unusual for data from individual chamber experiments to fall outside of the ambient range because ambient aerosol consists of a mixture from many precursors. The oxidation of naphthalene initiated by OH radicals leads to the formation of ring-opening products (e.g., formylcinnamaldedyhe) and organic acids.[22,23,38] Acidic compounds are usually produced from secondary or tertiary oxidation processes.

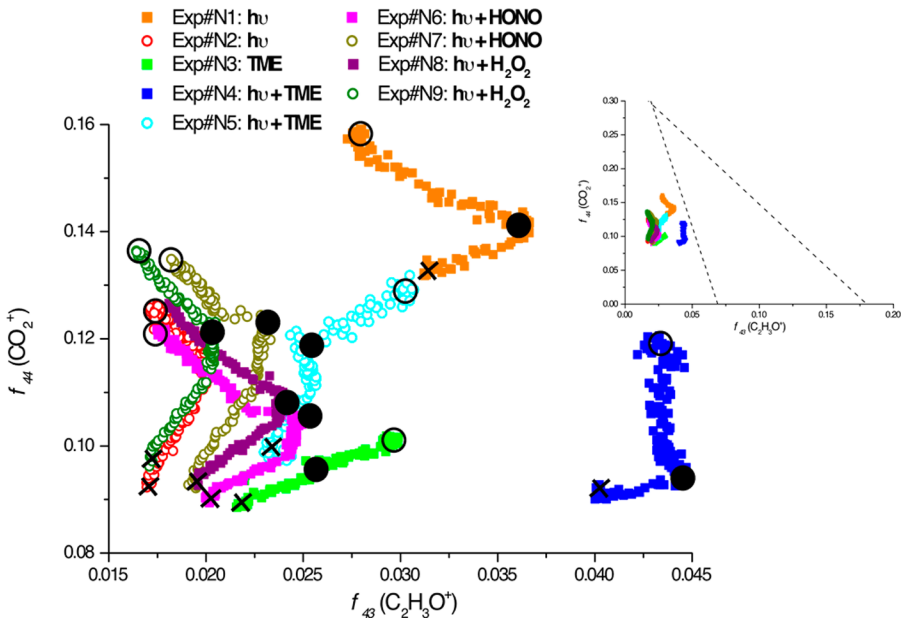

Figure 3. Triangle plot for SOA aging formed from naphthalene oxidation under different conditions. Cross, full, and open circles indicate SOA formation, start and end of aging processes, respectively (open and closed markers correspond to SOA formation performed with and without light, respectively). The inset shows the range reported in the literature for ambient data.

DOI: 10.1021/acs.est.5b00442
Environ. Sci. Technol. 2015, 49, 5407−5416

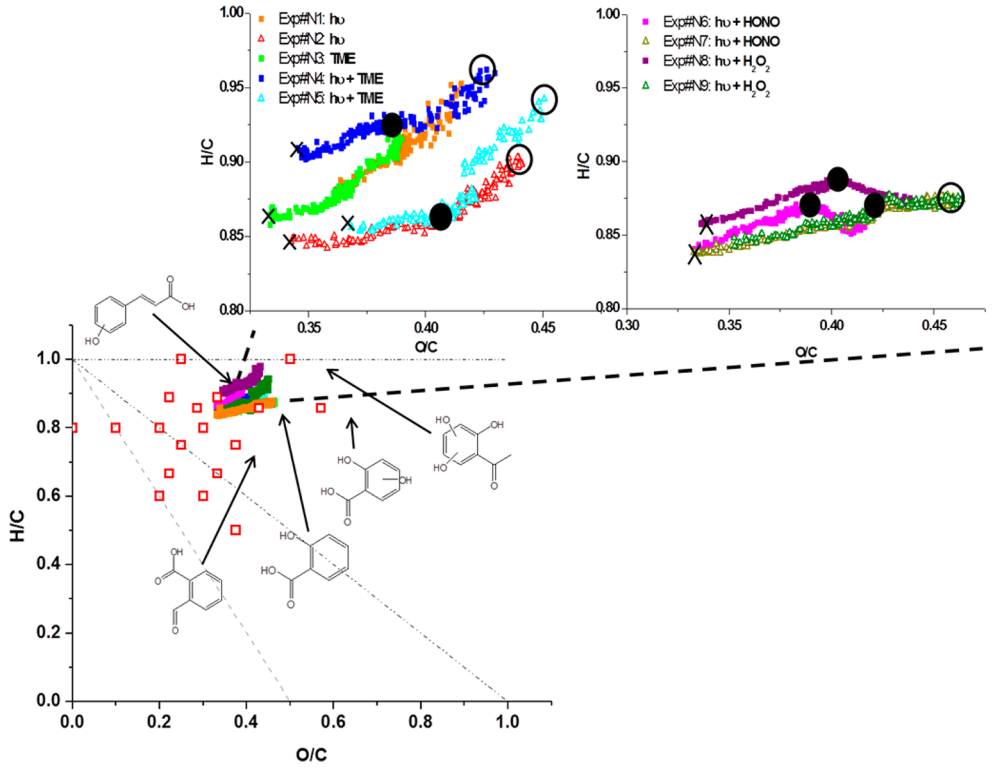

Figure 4. Van Krevelen diagram and a zoom box for aging of SOA from naphthalene oxidation under different conditions. Individual identified SOA products in the particulate phase and some proposed structures for the main acids identified are shown as open red squares, while the bulk SOA evolution for each experiment is shown as filled colored symbols. Growth in O/C with stable H/C (slope = 0) is consistent with alcohol or hydroxyperoxide formation. The initial period is likely governed by the condensation of early generation semi volatile products. For each case the initial period of SOA formation extends from the cross to the full circle, and the aging period then extends to the open circle. Data plotted with open and closed symbols correspond to SOA formation performed with and without UV light, respectively.

In the case of naphthalene photooxidation, different studies have demonstrated the formation of semivolatile organic compounds. Formation of identified compounds in the particulate phase (described below), such as formylcinnamaldehyde, can explain the evolution of the SOA bulk composition and also the SOA mass increase (SI Figure S5). Formation of secondary or tertiary products (like acids) in the gas phase followed by their partitioning into the particulate phase could explain both the increase of f_{44} and decrease of f_{43}. Moreover, an increase of aerosol mass was observed that seems to be correlated with the bulk evolution of the SOA (SI Figure S5). Indeed, the highest observed mass increases match with the experiments, where the respective increase and decrease of f_{44} and f_{43} are very pronounced. High concentrations of acidic compounds in the particle phase could explain the shift observed in the case of naphthalene SOA formation. Highly oxygenated products were formed during the aging experiments described here, resulting in an increase of f_{44} (CO_2^+) coupled with a decrease of f_{43} ($C_2H_3O^+$). In particular, this trend was very pronounced during aging reactions in the presence of UV light. Aging by OH radicals formed in darkness (Exp#N3) caused only a modest increase in f_{44} during the aging process. Other aromatics produce similar effects. The same tendency was observed during SOA aging with benzene as SOA precursor: highly oxidized compounds were produced during the aging processes. The authors demonstrated substantial production of carboxylic acids in the particulate phase to explain the growing f_{44}.[27,37]

We present a van Krevelen diagram (O/C vs H/C) Figure 4 to further constrain the evolution of the SOA during formation and aging.[7] The O/C ratio of SOA is commonly used as a tracer for atmospheric aging processes.[3,11] An increase of the O/C ratio for organic components is indicative of continuous oxygenation during experiments. In the van Krevelen diagrams, the gray dotted horizontal line represents evolution of the particulate phase composition leading to the formation of alcohols or peroxides. The black dotted straight line (with a slope of −1) is indicative of formation of acid or hydroxycarbonyl constituents in the SOA. Finally, the gray dotted straight line (with a slope of −2) corresponds to ketones or aldehydes.[7,37] Unseen gas-phase fragmentation products can influence the interpretation—for example, elimination of CO_2 can result in an apparent increase of H/C in the condensed phase products.

The data presented here include the complete reaction of naphthalene for all experiments, followed by various aging processes. In Figure 4, we plot both specific observed compounds (i.e., acids) and the bulk SOA composition for each experiment. In all experiments, the O/C ratio of the SOA increased significantly with time during both formation and aging, whereas the H/C ratio usually increased slightly. The identified acids and SOA bulk composition are consistent; this is notable because the specific products are identified at high masses (>100 amu) in the AMS spectra while the bulk O/C and H/C are determined almost entirely by very small fragments (m/z = 43, 44, etc.).

The first step in naphthalene oxidation is insertion of OH into the aromatic ring. In some cases, subsequent ring opening involves H atom shifts and thus the overall H/C increases due to the added OH. As presented in SI Table S3, half of the

DOI: 10.1021/acs.est.5b00442
Environ. Sci. Technol. 2015, 49, 5407−5416

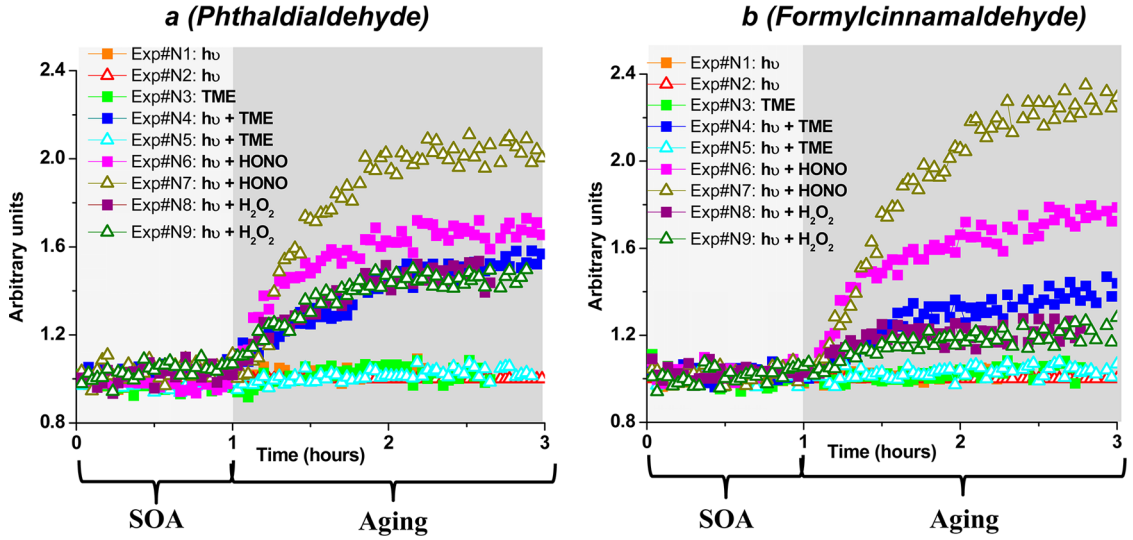

Figure 5. Evolution of phthaldialdehyde (a) and formylcinnamaldehyde (b) for different aging processes under different conditions. Signals are normalized using Exp#N2; aging (UV illumination or introduction OH radical precursors) started at t_0 = 1 h. Open and closed markers correspond to SOA formation performed with and without UV light, respectively.

naphthalene SOA products identified in this work exhibit a H/C ratio higher than the naphthalene. It is consistent with previous work where the main products from the photooxidation of naphthalene have a similar H/C ratio as the VOC.[23] Further SOA formation results from the generation of ketones or aldehydes followed by oxidation processes of carbonyl moieties to produce acidic compounds, leading to more oxidized organic aerosol.[23] The combination of OH insertion and acid formation results in a relatively flat H/C profile accompanied by a significant increase in O/C. Such results are in good agreement with those reported for the photooxidation of naphthalene in a previous study by Chhabra et al.[27]

The different aging processes caused different evolution in the bulk SOA, as shown in Figure 4. Due to the presence of many acidic compounds, hydration might be an important process (e.g., explaining the formation of phthalic acid) as reported in a previous study;[23] thus water may play a major role but we cannot conclude that definitively. Hydration appears on the van Krevelen diagram with a positive slope, corresponding to zero net change in the carbon oxidation state.[8] No systematic impact of UV light was observed during experiments Exp#N1 to Exp#N5. Functionalization involves the addition of oxygenated functional groups to a molecule without modification of carbon number, meaning that O/C ratio increases during such aging processes.[13] Moreover, the increase of f_{44} and the decrease of f_{43} coupled with an aerosol mass increase also indicate functionalization processes in the organic aerosol. In the case of aging processes involving HONO (Exp#N6 and Exp#N7) and H_2O_2 (Exp#N8 and Exp#N9) as OH precursors, the evolution of organic materials was different. When SOA was formed from naphthalene in darkness, the aging slopes were close to −0.5 (−0.5 and −0.6 for Exp#N6 and Exp#N8, respectively) indicating dominance of acid or hydroxycarbonyl formation during the oxidation processes.[7,39] Conversely, when SOA was produced in the presence of light (Exp#N7 and Exp#N9), the oxidation of organic aerosol was dominated by alcohol or peroxide formation (with a slope close to zero). Broadly, UV light or/and OH radicals alone do not seem to have a large impact on the bulk composition of the organic aerosol derived from naphthalene. However, the presence of either HO_2 or NO_x involved different oxidation pathways that may favor for instance the formation of either carboxylic acids or alkylnitrates/peroxynitrates, which is consistent with branching chemistry associated with peroxy radicals.[40] Peroxy radicals may also be involved in photolysis processes like ozone formation. A recent study[41] demonstrates the photooxidation of peroxy radicals; reverse addition, radical loss or isomerization processes are the possible reactions arising from photolysis. Even if it is difficult to conclude about such processes in our system, RO_2 photolysis (photoexcitation or photodissociation) may have to be considered on the further reactivity of RO_2 with NO or HO_2.

Aging Evolution of Particulate Naphthalene Products. After SOA formation from naphthalene we observed no subsequent evolution of identified products during aging in experiments Exp#N1, N2, N3, and N5. However, during experiments Exp#N4, N6, N7, N8, and N9 in the presence of OH radicals and light, we observed formation of several secondary products (reported in SI Table S3). Figure 5 presents the evolution of phthaldialdehyde (a) and formylcinnamaldehyde (b) for the different aging processes. Signals are normalized to that obtained in the absence of aging (Exp#N2). Experiments N6 and N7, in which OH was produced by HONO photolysis, showed the most dramatic increase in the secondary product concentrations and also the most dramatic increase in SOA mass during aging (SI Figure S5). This is consistent with bulk SOA aging experiments on α-pinene SOA using HONO photolysis[9] and is at least in part due to the high steady-state OH concentrations (>10^7 cm^{-3}) produced by this source.

Both phthaldialdehyde and formylcinnamaldehyde gas-phase chemistry with OH radicals, ozone, or in the presence of UV light have been described in the literature.[38,42] Some ring-opening products from naphthalene oxidation (e.g., formylcinnamaldehyde) have double bonds and therefore may react with ozone. For example, Atkinson's group reported the gas-phase rate constant for formylcinnamaldehyde plus ozone (1.8×10^{-18} cm^3 $molecule^{-1}$ s^{-1}) as well as its photolysis.[42] In this work, no ozonolysis reaction was observed in the heteroge-

DOI: 10.1021/acs.est.5b00442
Environ. Sci. Technol. 2015, 49, 5407−5416

neous phase. Due to the large concentration of ozone used in this study (i.e., 2 ppm), the lack of homogeneous or heterogeneous ozonation of products is surprising, as heterogeneous ozone oxidation has been demonstrated in many previous studies.[43,44] However, it is also known that heterogeneous loss of compounds such as oleic acid can be substantially diminished in particles consisting of complex organic mixtures.[44−47] The apparent stability of products with C═C double bonds reported here is consistent with formation of aerosols with low diffusivity of ozone into the particles (as well as slow diffusion of reactive products from the particle bulk to the surface).[48,49]

SOA Aging from Acenaphthylene Ozonolysis. In SI Figures S6 and S7, a van Krevelen diagram is presented to show data obtained during acenaphthylene ozonolysis and SOA aging. The evolution of the aerosol composition was different from that for naphthalene. Results show an increase of the O/C ratio during aging processes coupled to a global decreased of the H/C ratio. Although the incubation period was designed to assess "fresh" SOA, there was clearly chemical evolution of acenaphthylene ozonolysis SOA in the presence of UV light. Specific compounds allow us to constrain this chemistry. The constant increase of 1,8-naphthalic anhydride (**Product 7**) is suggestive of OH-radical chemistry. As demonstrated in previous publications,[26,30] 1,8-naphthalic anhydride is a secondary product from the oxidation of naphthalene-1,8-dicarbaldehyde (**Product 6**). The reaction is initiated by the H atom abstraction from the aldehyde functional group followed by the addition of O_2 to form a peroxy radical or by the cyclization of the radical formed by the H atom abstraction.[30,50] A peroxy radical could also be involved in 1,8-naphthalic anhydride formation by isomerization/cyclization.[30] Therefore, OH radicals present in the chamber may have various origins, but the most likely is $O(^1D)$ from ozone photolysis in the spin-forbidden region between 300 and 400 nm.[51,52] Moreover, photolysis of oxidized compounds such as peroxides is known to form OH radicals and to be involved in the formation of highly oxidized products. Nonetheless, based on the low concentration experiments where 50 ppb of ozone was used to initiate SOA formation in the presence of light, no significant depletion of oxygenated products was observed and thus, formation of OH radicals by ozone photolysis is assumed to be the main process to explain the observed chemical evolution. Direct photolysis of carbonyl functional groups could also participate in the depletion of primary products and the production of secondary products. For example, the aldehyde functional group may be photodissociated via different pathways. In the case of aliphatic aldehydes, one pathway may involve C—H bond cleavage from the CHO group. Wang et al.[53] studied phthaldialdehyde photolysis ($C_8H_6O_2$, produced during naphthalene photooxidation), and they concluded that phthalic anhydride ($C_8H_4O_3$) is one of the main products arising from the photolysis steps. However, the evolution of acenaphthylene SOA under UV illumination shown in Figure 2 cannot be explained by photolysis alone. By comparison with naphthalene experiments, no photolysis processes of carbonyl products such as phthaldialdehyde, were evident. Observed depletion of some of the acenaphthylene products appear driven by secondary oxidation arising from OH radicals produce from secondary processes like ozone photolysis. Although the absorption cross sections for most acenaphthylene products are unknown, it is reasonable to assume that they are at least as photosensitive as products arising from naphthalene oxidation; photolysis appears, however, negligible. Also, the physical properties of SOA formed from naphthalene and acenaphthylene appear different, especially due to the absence of photolysis process of naphthalene products. As proposed by Wong et al.[49] with α-pinene, in viscous semisolid material, the slow diffusion of naphthalene SOA photooxidation products could favor their recombination and reduce the quantum yields from photolysis even if they absorb UV light.

The van Krevelen analysis (SI Figure S7) shows that the composition of SOA generated in the presence of UV light (Exp#A4, A5, A7, A9) differs from that formed in darkness. The bulk composition of SOA formed in the dark showed very little evolution during formation, while the presence of UV light induced fragmentation and/or functionalization processes, driving a decrease in the H/C ratio and an increase in the O/C ratio. Different types of aging (OH radical reaction, photolysis, or both) caused markedly different changes to the SOA composition. The only presence of OH radicals during aging experiments Exp#A2 and A4, was associated with an increase of both the H/C and O/C ratios. The slight positive slope (+0.4 and +0.5 for Exp#A2 and A4, respectively) seems to be due to a fragmentation process, which is observed by a slight increase of $C_{11}H_xO_x$ products (such as naphthaldehyde, hydroxyl-naphthaldehyde and oxaacenaphthylene-2-one), while concentrations of C_{12} products appeared stable during both experiments. Due to carbon depletion, both O/C and H/C ratios increase. UV light alone induced, as previously described, a significant decrease of H/C and an increase of the O/C ratio (Exp#A1). The combination of OH radicals and UV light caused changes similar to those previously described for naphthalene (e.g., oxidation of organic aerosol was dominated by alcohol or peroxide formation with a slope close to zero). However, in these cases (Exp#A1 and A3), the van Krevelen slopes were somewhat different from other aging experiments, suggesting that the presence of HO_2 or NO_x, as identified for naphthalene experiments, involved different oxidation pathways (favoring the formation of carboxylic acid).[40]

In general, functionalization pathways seem to be favored due first to the specific structure of acenaphthylene (i.e., the unsaturated cyclopenta-fused ring). Indeed, due to the presence of stable aromatic rings, fragmentation appeared to be difficult compared to the case of aliphatic compounds. Second, during aging, SOA mass shown increases for most experiments as already observed for naphthalene experiments. Finally, during all different experiments, the formation of $C_{12}H_xO_x$ products seems to be favored, as previously described for 1,8-naphthalic anhydride (**Product 7**, SI Table S2), which is one of the most abundant compounds identified in the particulate phase, demonstrating the potential importance of functionalization during acenaphthylene oxidation. Moreover, SOA from acenaphthylene ozonolysis has a relatively low O/C ratio, suggesting that functionalization was the most important oxidation pathway.[8] Fragmentation could become important for later generations of oxidation. The final O/C ratio obtained was around 0.4 at the end of aging processes, consistent with moderately oxidized aerosol.[8]

Aging Evolution of Particulate Acenaphthylene Products. Specific products reported in SI Table S2 after acenaphthylene ozonolysis can be separated in two different groups. First, group 1 (**Products 1**, **3**, and **7**) contains compounds presenting the same temporal trend, sometimes increasing and sometimes decreasing during aging. The evolution of the relative concentration of 1,8-naphthalic

DOI: 10.1021/acs.est.5b00442
Environ. Sci. Technol. 2015, 49, 5407−5416

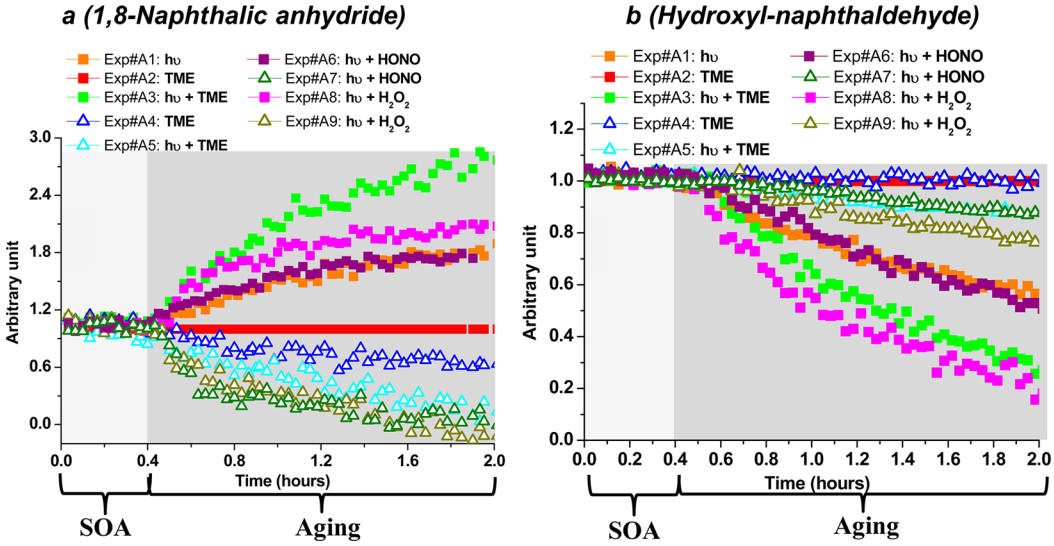

Figure 6. Evolution of 1,8-naphthalic anhydride (a) and of hydroxyl-naphthaldehyde (b) for different aging processes of SOA formed from acenaphthylene. Open and closed markers correspond to SOA formation performed with and without light, respectively. Signals are normalized using Exp#A2; aging with UV light or OH started at t_0 = 0.4 h.

anhydride (**Product 7**) is presented in Figure 6 as representative of this group. As previously discussed, some compounds were either consumed or generated when UV light was present during both SOA formation and aging. During aging processes, products of group 1 were formed if the initial SOA was produced in darkness, whereas the same products were depleted if the initial SOA was generated in the presence of UV light. For group 2 (**Products 2**, **4**, **5**, **6**, and **8**), the effect of photolysis during aging was evident in all the cases (i.e., fresh SOA generated in the presence or in absence of lights). However, if the aging was conducted in darkness (Exp#A2 and A4), then we observed no degradation of products from group 2. We show hydroxyl-naphthaldehyde (**Product 4**) in Figure 6b to represent this group. The loss of the different species was less pronounced when the SOA was generated in the presence of UV light. Indeed, as discussed above, compounds in group 2 were depleted during the oxidation of acenaphthylene in the presence of UV light. The product concentrations during aging were much lower and thus, the consumption of these compounds was smaller in the case of SOA formed under UV illumination (Exp#A5, A7, A9). In the case of SOA formed in darkness, the degradation of primary products (from group 2) was more substantial. The depletion was even more pronounced when the OH radical concentration was high (using HONO or TME, in the presence of UV light).

As discussed above, the reactivity of the first-generation particulate products was strongly influenced by UV light. Although compounds from group 1 were directly produced during acenaphthylene ozonolysis, they may also have been generated as secondary products following the photooxidation of primary products by OH in the presence of UV light.[25,26,30] For example, oxaacenaphthylene-2-one (**Product 3**) and 1,8-naphthalic anhydride (**Product 7**) may be formed by the oxidation of naphthalene-1,8-dicarbaldehyde (**Product 6**) initiated by OH radicals. The increased reactivity of condensed-phase products is consistent with a reduced viscosity SOA formed from acenaphthylene compared with SOA formed from naphthalene. Indeed, gaseous and particulate phase interactions appear to be more pronounced. For example, the correlated increase and decrease of products of groups 1 and 2, respectively, support this assumption. Therefore, aging pathways may this time occur in both homogeneous (as for the naphthalene) and heterogeneous phases. Globally, when no significant change in the concentration of specific particulate-phase products was observed, there was a corresponding increase of H/C and O/C ratios (SI Figure S7). This trend is evident for experiments Exp#A2 and Exp#A4, which did show a significant increase in total SOA mass during aging, evidently from later-generation products.

Aging chemistry of SOA formed from PAH oxidation is clearly facile on subday time scales. The PAHs provide an unusual opportunity to observe aging chemistry with molecular-level detail using instruments designed for bulk SOA characterization such as the Aerosol Mass Spectrometer. This has allowed us to elucidate the oxidation mechanisms over several generations for both naphthalene oxidation and acenaphthylene ozonolysis.

■ ASSOCIATED CONTENT

Supporting Information

Experimental setup and analysis techniques; experimental conditions are summarized and described in Table S1. Tables S2 and S3 present identified products in particle phase during acenaphthylene ozonolysis and naphthalene oxidation, respectively. Figure S1 presents mass spectra obtained during acenaphthylene oxidation and corresponding mass fragments of identified products. Figures S2 and S3 detail all fit of all identified fragments during naphthalene and acenaphthylene oxidation, respectively. Figure S4 is a time profile of four SOA naphthalene oxidation products. Figure S5 shows organic aerosol mass evolution during the different aging processes for SOA formed from naphthalene oxidation. Figures S6 and S7 present a van Krevelen diagram for acenaphthylene ozonolysis. This material is available free of charge via the Internet at http://pubs.acs.org.

■ AUTHOR INFORMATION

Corresponding Authors

*Phone: +1-412-268-7139; e-mail: nmd@andrew.cmu.edu.

DOI: 10.1021/acs.est.5b00442
Environ. Sci. Technol. 2015, 49, 5407−5416

*Phone: +33 5 4000 6350; e-mail: e.villenave@epoc.u-bordeaux1.fr.

Present Address

[‖]Department of Environmental Sciences and Engineering, Gillings School of Global Public Health, The University of North Carolina at Chapel Hill, Chapel Hill, North Carolina 27599, United States.

Notes

The authors declare no competing financial interest.

■ ACKNOWLEDGMENTS

The authors wish to thank the French Agency for Environment and Energy Management (ADEME) for their financial support. This study has been carried out with financial support from the French National Research Agency (ANR) in the frame of the Investments for the future Program, within the Cluster of Excellence COTE (ANR-10-LABX-45). CMU researchers were supported by grant NSF AGS1136479. The HR AMS was purchased with NSF MRI funding (CBET9022643) and the Wallace Foundation.

■ REFERENCES

(1) Pope, C. A., III; Dockery, D. W. Health effects of fine particulate air pollution: lines that connect. *J. Air Waste Manage. Assoc.* **2006**, *56* (6), 709−742.

(2) Hallquist, M.; Wenger, J. C.; Baltensperger, U.; Rudich, Y.; Simpson, D.; Claeys, M.; Dommen, J.; Donahue, N. M.; George, C.; Goldstein, A. H.; Hamilton, J. F.; Herrmann, H.; Hoffmann, T.; Iinuma, Y.; Jang, M.; Jenkin, M. E.; Jimenez, J. L.; Kiendler-Scharr, A.; Maenhaut, W.; McFiggans, G.; Mentel, Th.F.; Monod, A.; Prévôt, A. S. H.; Seinfeld, J. H.; Surratt, J. D.; Szmigielski, R.; Wildt, J. The formation, properties and impact of secondary organic aerosol: current and emerging issues. *Atmos. Chem. Phys.* **2009**, *9* (14), 5155−5236.

(3) Jimenez, J. L.; Canagaratna, M. R.; Donahue, N. M.; Prévôt, A. S. H.; Zhang, Q.; Kroll, J. H.; DeCarlo, P. F.; Allan, J. D.; Coe, H.; Ng, N. L.; Aiken, A. C.; Docherty, K. S.; Ulbrich, I. M.; Grieshop, A. P.; Robinson, A. L.; Duplissy, J.; Smith, J. D.; Wilson, K. R.; Lanz, V. A.; Hueglin, C.; Sun, Y. L.; Tian, J.; Laaksonen, A.; Raatikainen, T.; Rautiainen, J.; Vaattovaara, P.; Ehn, M.; Kulmala, M.; Tomlinson, J. M.; Collins, D. R.; Cubison, M. J.; Dunlea, E. J.; Huffman, J. A.; Onasch, T. B.; Alfarra, M. R.; Williams, P. I.; Bower, K.; Kondo, Y.; Schneider, J.; Drewnick, F.; Borrmann, S.; Weimer, S.; Demerjian, K.; Salcedo, D.; Cottrell, L.; Griffin, R.; Takami, A.; Miyoshi, T.; Hatakeyama, S.; Shimono, A.; Sun, J. Y.; Zhang, Y. M.; Dzepina, K.; Kimmel, J. R.; Sueper, D.; Jayne, J. T.; Herndon, S. C.; Trimborn, A. M.; Williams, L. R.; Wood, E. C.; Middlebrook, A. M.; Kolb, C. E.; Baltensperger, U.; Worsnop, D. R. Evolution of organic aerosols in the atmosphere. *Science* **2009**, *326* (5959), 1525−1529.

(4) Ng, N. L.; Canagaratna, M. R.; Zhang, Q.; Jimenez, J. L.; Tian, J.; Ulbrich, I. M.; Kroll, J. H.; Docherty, K. S.; Chhabra, P. S.; Bahreini, R.; Murphy, S. M.; Seinfeld, J. H.; Hildebrandt, L.; Donahue, N. M.; DeCarlo, P. F.; Lanz, V. A.; Prévôt, A. S. H.; Dinar, E.; Rudich, Y.; Worsnop, D. R. Organic aerosol components observed in Northern Hemispheric datasets from aerosol mass spectrometry. *Atmos. Chem. Phys.* **2010**, *10* (10), 4625−4641.

(5) Rudich, Y.; Donahue, N. M.; Mentel, T. F. Aging of organic aerosol: Bridging the gap between laboratory and field studies. *Annu. Rev. Phys. Chem.* **2007**, *58*, 321−352.

(6) Chhabra, P. S.; Flagan, R. C.; Seinfeld, J. H. Elemental analysis of chamber organic aerosol using an aerodyne high-resolution aerosol mass spectrometer. *Atmos. Chem. Phys.* **2010**, *10* (9), 4111−4131.

(7) Heald, C. L.; Kroll, J. H.; Jimenez, J. L.; Docherty, K. S.; DeCarlo, P. F.; Aiken, A. C.; Chen, Q.; Martin, S. T.; Farmer, D. K.; Artaxo, P. A simplified description of the evolution of organic aerosol composition in the atmosphere. *Geophys. Res. Lett.* **2010**, *37* (8), L08803.

(8) Kroll, J. H.; Smith, J. D.; Che, D. L.; Kessler, S. H.; Worsnop, D. R.; Wilson, K. R. Measurement of fragmentation and functionalization pathways in the heterogeneous oxidation of oxidized organic aerosol. *Phys. Chem. Chem. Phys.* **2009**, *11* (36), 8005−8014.

(9) Donahue, N. M.; Henry, K. M.; Mentel, T. F.; Kiendler-Scharr, A.; Spindler, C.; Bohn, B.; Brauers, T.; Dorn, H. P.; Fuchs, H.; Tillmann, R.; Wahner, A.; Saathoff, H.; Naumann, K.-H.; Mohler, O.; Leisner, T.; Muller, L.; Reinnig, M.-C.; Hoffmann, T.; Salo, K.; Hallquist, M.; Frosch, M.; Bilde, M.; Tritscher, T.; Barmet, P.; Praplan, A. P.; DeCarlo, P. F.; Dommen, J.; Prévôt, A. S. H.; Baltensperger, U. Aging of biogenic secondary organic aerosol via gas-phase OH radical reactions. *Proc. Natl. Acad. Sci. U. S. A.* **2012**, *109* (34), 13503−13508.

(10) Henry, K. M.; Donahue, N. M. Photochemical aging of α-pinene secondary organic aerosol: effects of OH radical sources and photolysis. *J. Phys. Chem. A* **2012**, *116* (24), 5932−5940.

(11) Lambe, A. T.; Onasch, T. B.; Croasdale, D. R.; Wright, J. P.; Martin, A. T.; Franklin, J. P.; Massoli, P.; Kroll, J. H.; Canagaratna, M. R.; Brune, W. H.; Worsnop, D. R.; Davidovits, P. Transitions from functionalization to fragmentation reactions of laboratory secondary organic aerosol (SOA) generated from the OH oxidation of alkane precursors. *Environ. Sci. Technol.* **2012**, *46* (10), 5430−5437.

(12) Sato, K.; Takami, A.; Kato, Y.; Seta, T.; Fujitani, Y.; Hikida, T.; Shimono, A.; Imamura, T. AMS and LC/MS analyses of SOA from the photooxidation of benzene and 1,3,5-trimethylbenzene in the presence of NO_x: effects of chemical structure on SOA aging. *Atmos. Chem. Phys.* **2012**, *12* (10), 4667−4682.

(13) Chacon-Madrid, H. J.; Donahue, N. M. Fragmentation vs. functionalization: chemical aging and organic aerosol formation. *Atmos. Chem. Phys.* **2011**, *11* (20), 10553−10563.

(14) Kroll, J. H.; Seinfeld, J. H. Chemistry of secondary organic aerosol: formation and evolution of low-volatility organics in the atmosphere. *Atmos. Environ.* **2008**, *42* (16), 3593−3624.

(15) Tritscher, T.; Dommen, J.; DeCarlo, P. F.; Gysel, M.; Barmet, P. B.; Praplan, A. P.; Weingartner, E.; Prévôt, A. S. H.; Riipinen, I.; Donahue, N. M.; Baltensperger, U. Volatility and hygroscopicity of aging secondary organic aerosol in a smog chamber. *Atmos. Chem. Phys.* **2011**, *11* (22), 11477−11496.

(16) Salo, K.; Hallquist, M.; Jonsson, A. M.; Saathoff, H.; Naumann, K.-H.; Spindler, C.; Tillmann, R.; Fuchs, H.; Bohn, B.; Rubach, F.; Mentel, Th.F.; Muller, L.; Reinig, M.; Hoffmann, T.; Donahue, N. M. Volatility of secondary organic aerosol during OH radical induced ageing. *Atmos. Chem. Phys.* **2011**, *11* (21), 11055−11067.

(17) Tkacik, D. S.; Presto, A. A.; Donahue, N. M.; Robinson, A. L. Secondary organic aerosol formation from intermediate-volatility organic compounds: cyclic, linear, and branched alkanes. *Environ. Sci. Technol.* **2012**, *46* (16), 8773−8781.

(18) Atkinson, R.; Arey, J. Atmospheric chemistry of gas-phase polycyclic aromatic hydrocarbons: Formation of atmospheric mutagens. *Environ. Health Presp.* **1994**, *102* (suppl. 4), 117−126.

(19) Keyte, I. J.; Harrison, R. M.; Lammel, G. Chemical reactivity and long-range transport potential of polycyclic aromatic hydrocarbons—a review. *Chem. Soc. Rev.* **2013**, *42* (24), 9333−9391.

(20) Robinson, A. L.; Subramanian, R.; Donahue, N. M.; Bernardo-Bricker, A.; Rogge, W. F. Source apportionment of molecular markers and organic aerosol-1. Polycyclic aromatic hydrocarbons and methodology for data visualization. *Environ. Sci. Technol.* **2006**, *40* (24), 7803−7810.

(21) Chan, A. W. H.; Kautzman, K. E.; Chhabra, P. S.; Surratt, J. D.; Chan, M. N.; Crounse, J. D.; Kürten, A.; Wennberg, P. O.; Flagan, R. C.; Seinfeld, J. H. Secondary organic aerosol formation from photooxidation of naphthalene and alkylnaphthalenes: implications for oxidation of intermediate volatility organic compounds (IVOCs). *Atmos. Chem. Phys.* **2009**, *9* (9), 3049−3060.

(22) Lee, J. Y.; Lane, D. A. Unique products from the reaction of naphthalene with the hydroxyl radical. *Atmos. Environ.* **2009**, *43* (32), 4886−4893.

(23) Kautzman, K. E.; Surratt, J. D.; Chan, M. N.; Chan, A. W. H.; Hersey, S. P.; Chhabra, P. S.; Dalleska, N. F.; Wennberg, P. O.; Flagan, R. C.; Seinfeld, J. H. Chemical composition of gas- and aerosol-phase

DOI: 10.1021/acs.est.5b00442
Environ. Sci. Technol. 2015, 49, 5407−5416

products from the photooxidation of naphthalene. *J. Phys. Chem. A* **2010**, *114* (2), 913−934.
(24) Kleindienst, T. E.; Jaoui, M.; Lewandowski, M.; Offenberg, J. H.; Docherty, K. S. The formation of SOA and chemical tracer compounds from the photooxidation of naphthalene and its methyl analogs in the presence and absence of nitrogen oxide. *Atmos. Chem. Phys.* **2012**, *12* (18), 8711−8726.
(25) Riva, M.; Healy, R. M.; Tomaz S.; Flaud, P.-M.; Perraudin, E.; Wenger, J. C.; Villenave, E. Composition of gas and particulate phase products from the ozonolysis of acenaphthylene. *Submitted to Atmos. Environ.*
(26) Riva, M. *Caractérisation d'une nouvelle voie de formation des aérosols organiques secondaires (AOS) dans l'atmosphère: Rôle des précurseurs polyaromatiques*. PhD thesis, University of Bordeaux, France,(2013).
(27) Chhabra, P. S.; Ng, N. L.; Canagaratna, M. R.; Corrigan, A. L.; Russell, L. M.; Worsnop, D. R.; Flagan, R. C.; Seinfeld, J. H. Elemental composition and oxidation of chamber organic aerosol. *Atmos. Chem. Phys.* **2011**, *11* (17), 8827−8845.
(28) Saukko, E.; Lambe, A. T.; Massoli, P.; Koop, T.; Wright, J. P.; Croasdale, D. R.; Pedernera, D. A.; Onasch, T. B.; Laaksonen, A.; Davidovits, P.; Worsnop, D. R.; Virtanen, A. Humidity-dependent phase state of SOA particles from biogenic and anthropogenic precursors. *Atmos. Chem. Phys.* **2012**, *12* (16), 7517−7529.
(29) Pye, H. O. T.; Pouliot, G. A. Modeling the role of alkanes, polycyclic aromatic hydrocarbons, and their oligomers in secondary organic aerosol formation. *Environ. Sci. Technol.* **2012**, *46* (11), 6041−6047.
(30) Zhou, S.; Wenger, J. C. Kinetics and products of the gas-phase reactions of acenaphthylene with hydroxyl radicals, nitrate radicals and ozone. *Atmos. Environ.* **2013**, *75* (71), 103−112.
(31) Hildebrandt, L.; Donahue, N. M.; Pandis, S. N. High formation of secondary organic aerosol from the photo-oxidation of toluene. *Atmos. Chem. Phys.* **2009**, *9* (9), 2973−2986.
(32) Lambe, A. T.; Zhang, J.; Sage, A. M.; Donahue, N. M. Controlled OH radical production via ozone-alkene reactions for use in aerosol aging studies. *Environ. Sci. Technol.* **2007**, *41* (7), 2357−2363.
(33) DeCarlo, P. F.; Kimmel, J. R.; Trimbom, A.; Northway, M. J.; Jayne, J. T.; Aiken, A. C.; Gonin, M.; Fuhrer, K.; Horvath, T.; Docherty, K. S.; Worsnop, D. R.; Jimenez, J. L. Field-deployable, high resolution, time-of-flight aerosol mass spectrometer. *Anal. Chem.* **2006**, *78* (24), 8281−8289.
(34) Dzepina, K.; Arey, J.; Marr, L. C.; Worsnop, D. R.; Salcedo, D.; Zhang, Q.; Onasch, T. B.; Molina, L. T.; Molina, M. J.; Jimenez, J. L. Detection of particle-phase polycyclic aromatic hydrocarbons in Mexico City using an aerosol mass spectrometer. *Int. J. Mass. Spectrom.* **2007**, *263* (2), 152−170.
(35) Atkinson, R.; Aschmann, S. M.; Pitts, J. N. Kinetics of the reactions of naphthalene and biphenyl with OH radicals and with O_3 at 294 ± 1 K. *Environ. Sci. Technol.* **1984**, *18* (2), 110−113.
(36) Calvert, J. G.; Atkinson, R.; Becker, K. H.; Kamens, R. M.; Seinfeld, J. H.; Wallington, T. J.; Yarwood, G. *The Mechanisms of Atmospheric Oxidation of Aromatic Hydrocarbons*; Oxford University Press: Oxford, U.K., 2002; pp 556.
(37) Sato, K.; Takami, A.; Kato, Y.; Seta, T.; Fujitani, Y.; Hikida, T.; Shimono, A.; Imamura, T. AMS and LC/MS analyses of SOA from the photooxidation of benzene and 1,3,5-trimethylbenzene in the presence of NO_x: effects of chemical structure on SOA aging. *Atmos. Chem. Phys.* **2012**, *12* (11), 4667−4682.
(38) Nishino, N.; Arey, J.; Atkinson, R. Formation and reactions of 2-formylcinnamaldehyde in the OH radical-initiated reaction of naphthalene. *Environ. Sci. Technol.* **2009**, *43* (5), 1349−1353.
(39) Ng, N. L.; Canagaratna, M. R.; Jimenez, J. L.; Chhabra, P. S.; Seinfeld, J. H.; Worsnop, D. R. Changes in organic aerosol composition with aging inferred from aerosol mass spectra. *Atmos. Chem. Phys.* **2011**, *11* (13), 6465−6474.
(40) Ziemann, P. J.; Atkinson, R. Kinetics, products, and mechanisms of secondary organic aerosol formation. *Chem. Soc. Rev.* **2012**, *41* (19), 6582−6605.
(41) Kalafut-Pettibone, A. L.; Klems, J. P.; Burgess, D. R.; McGivern, W. S. Alkylperoxyl radical photochemistry in organic aerosol formation processes. *J. Phys. Chem. A* **2013**, *117* (51), 14141−14150.
(42) Aschmann, S. M.; Arey, J.; Atkinson, R. Study of the atmospheric chemistry of 2-formylcinnamaldehyde. *J. Phys. Chem. A* **2013**, *117* (33), 7876−7886.
(43) Perraudin, E.; Budzinski, H.; Villenave, E. Kinetic study of the reactions of ozone with polycyclic aromatic hydrocarbons adsorbed on atmospheric model particles. *J. Atmos. Chem.* **2007**, *56* (1), 57−82.
(44) Miet, K.; Budzinski, H.; Villenave, E. Heterogeneous reactions of ozone with pyrene, 1-hydroxypyrene and 1-nitropyrene adsorbed on particles. *Atmos. Environ.* **2009**, *43* (24), 3699−3707.
(45) Knopf, D. A.; Anthony, L. M.; Bertram, A. K. Reactive uptake of O_3 by multicomponent and multiphase mixtures containing oleic acid. *J. Phys. Chem. A* **2005**, *109* (25), 5579−5589.
(46) Huff Hartz, K. E.; Weitkamp, E. A.; Sage, A. M.; Donahue, N. M.; Robinson, A. L. Laboratory measurements of the oxidation kinetics of organic aerosol mixtures using a relative rate constants approach. *J. Geophys. Res.* **2007**, *112* (D4), D04204.
(47) Sage, A. M.; Weitkamp, E. A.; Robinson, A. L.; Donahue, N. M. Reactivity of oleic acid in organic particles: change in oxidant uptake and reaction stoichiometry with particle oxidation. *Phys. Chem. Chem. Phys.* **2009**, *11* (36), 7951−7962.
(48) Shiraiwa, M.; Ammann, M.; Koop, T.; Pöschl, U. Gas uptake and chemical aging of semisolid organic aerosol particles. *Proc. Natl. Acad. Sci.* **2011**, *108* (27), 11003−11008.
(49) Wong, J. P. S.; Zhou, S.; Abbatt, J. P. D. Changes in secondary organic aerosol composition and mass due to photolysis: relative humidity dependence. *J. Phys. Chem. A* **2014**.
(50) Bauer, D.; D'Ottone, L.; Hynes, A. J. O^1D quantum yields form O_3 photolysis in the near UV region between 305 and 375 nm. *Phys. Chem. Chem. Phys.* **2000**, *2* (1), 1421−1424.
(51) Matsumi, Y.; Comes, F. J.; Hancock, G.; Hofzumahaus, A.; Hynes, A. J.; Kawasaki, M.; Ravishankara, A. R. Quantum yields for production of $O(^1D)$ in the ultraviolet photolysis of ozone: recommendation based on evaluation of laboratory data. *J. Geophys. Res.* **2002**, *107* (D3), 1−12.
(52) Ng, N. L.; Canagaratna, M. R.; Jimenez, J. L.; Chhabra, P. S.; Seinfeld, J. H.; Worsnop, D. R. Changes in organic aerosol composition with aging inferred from aerosol mass spectra. *Atmos. Chem. Phys.* **2011**, *11* (13), 6465−6474.
(53) Wang, L.; Arey, J.; Atkinson, R. Kinetics and products of photolysis and reaction with OH radicals of a series of aromatic carbonyl compounds. *Environ. Sci. Technol.* **2006**, *40* (17), 5465−5471.

DOI: 10.1021/acs.est.5b00442
Environ. Sci. Technol. 2015, 49, 5407−5416